

## Alignment of isovalent impurity levels: Oxygen impurity in II-VI semiconductors

Jingbo Li and Su-Huai Wei

National Renewable Energy Laboratory, Golden, Colorado 80401, USA

(Received 21 December 2005; published 24 January 2006)

The isovalent oxygen impurity levels in the II-VI semiconductors ZnSe:O, ZnTe:O, and CdTe:O are studied using a method based on first-principles total energy and large scale charge patching band structure calculations. We find that, unlike the general expectation that these levels line up in an absolute energy scale, the positions of the isovalent  $a_1(\text{O})$  level depend sensitively on the local environment around the impurity, thus, the  $a_1(\text{O})$  levels align approximately only in the common-cation systems, whereas in the common-anion systems, the levels do not align. These general chemical trends also apply to other isovalent impurity systems.

DOI: [10.1103/PhysRevB.73.041201](https://doi.org/10.1103/PhysRevB.73.041201)

PACS number(s): 78.66.Hf, 71.15.-m, 71.55.-i

Isovalent impurity systems are those in which the substitutional atoms have the same number of valence electrons as the host atoms they replace. In most cases, the difference between the contribution of the core electronic structure of the isovalent impurity and the substituted host atom is not large, therefore, no bound states inside the forbidden band gap are expected. However, in some special cases when the chemical and size differences between the isovalent impurity and the substituted host atom are large, isovalent trap states can form.<sup>1</sup> Generally speaking,<sup>2</sup> when the electronegativity of the isovalent impurity is much larger than the host atom (e.g., GaP:N and ZnTe:O), the isovalent impurity level with  $a_1$  symmetry will form near the conduction band minimum (CBM), whereas when the electronegativity of the isovalent impurity is much smaller than the host atom (e.g., GaN:As and ZnS:Te), the isovalent impurity level with  $t_2$  symmetry will form near the valence band maximum.

The systems that present isovalent impurity levels have attracted much attention recently because these systems often exhibit drastic changes of their electrical and optical properties as a function of impurity concentration.<sup>3</sup> For example, although the band gap of GaN is significantly larger than that of GaAs, the band gap of GaAs:N will decrease by about 0.18 eV when only 1% of the As atoms is replaced by N.<sup>4</sup> Isovalent doping of GaP by N can also change the material from an indirect gap semiconductor to a quasidirect gap semiconductor with enhanced optical functionality.<sup>5</sup> These effects has opened up great potential in engineering the electrical and optical properties of a material without significant change to its structural properties.

Since the discovery of the isoelectronic trap state for semiconductors in the 1960s, much experimental and theoretical work has been done to understand the formation mechanism and position of such isovalent bound states.<sup>2-8</sup> Various models have been proposed. Hopfield *et al.*<sup>2</sup> emphasized on the different electronegativities between the isovalent impurity atom and the host atom. Allen<sup>6</sup> considered the lattice deformation potential effect resulting from the different sizes of impurity atoms. Phillips<sup>7</sup> further argued that electron polarization and screening can also play an important role, which can significantly reduce the binding energy. The most extensively studied systems to date are nitrogen doped GaAs and GaP. Absorption and photoluminescence excitation measurements show that in GaAs:N and GaP:N

the strongly localized isolated nitrogen-impurity levels exist near the CBM. In GaP:N this level appears at about 10 meV below the CBM,<sup>1</sup> whereas in GaAs:N, it appears as a sharp resonance at about 180 meV above CBM.<sup>8</sup> Using the calculated valence band offset<sup>9</sup> of 0.47 eV between GaP and GaAs and the fact that the band gaps of GaAs and GaP are 1.52 and 2.35 eV [Fig. 1(a)], respectively, we find that the localized N impurity level in GaP is only about 0.13 eV higher than that in GaAs in an absolute energy scale. Therefore, within theoretical and experimental uncertainty, N impurity levels tend to line up in these common-cation systems.

Similar experimental studies have also been done recently for isovalent impurity oxygen in II-VI semiconductors.<sup>10-13</sup> Yu and co-workers<sup>10</sup> reported that oxygen exhibits a deep impurity level inside the band gap of ZnTe at about 0.24 eV below the CBM at room temperature (RT), consistent with earlier experimental data,<sup>14</sup> which reported an oxygen level at about 0.4 eV below the CBM at low temperature in ZnTe. For ZnSe:O and CdTe:O, the measurements at RT and a fit to the two-band anticrossing model by Yu *et al.*<sup>11-13</sup> assigned the localized oxygen resonant states at approximately 0.22 eV and 0.4 eV, respectively, above CBM (or at about CBM+0.07 eV and CBM+0.25 eV, respectively, for ZnSe:O and CdTe:O at low temperature). In their fitting process, they assumed that the oxygen impurity levels in ZnSe and CdTe line up with that in ZnTe, although the derived valence band offsets are slightly different from the calculated valence band offsets [Fig. 1(b)].<sup>9</sup> This raised an interesting question about whether (or in what degree) the localized isovalent impurity level should line up in a group of semiconductors, and what determines the energy level positions.

Traditionally, one often assumes that a localized defect level in a group of semiconductors lines up in an absolute energy scale. Based on this assumption, the localized defect level has been used to derive the band offsets between different compounds.<sup>11,15</sup> It has also been used to estimate whether a particular dopant should be an acceptor or a donor in a group of compounds.<sup>16</sup> However, the uncertainty in these assumptions has never been calculated accurately and consistently in the past because of computational difficulties. For conventional local-density approximation (LDA) calculations, there are two major issues.

(1) The well-known LDA band gap error makes it difficult to locate the impurity level position in a semiconductor, es-

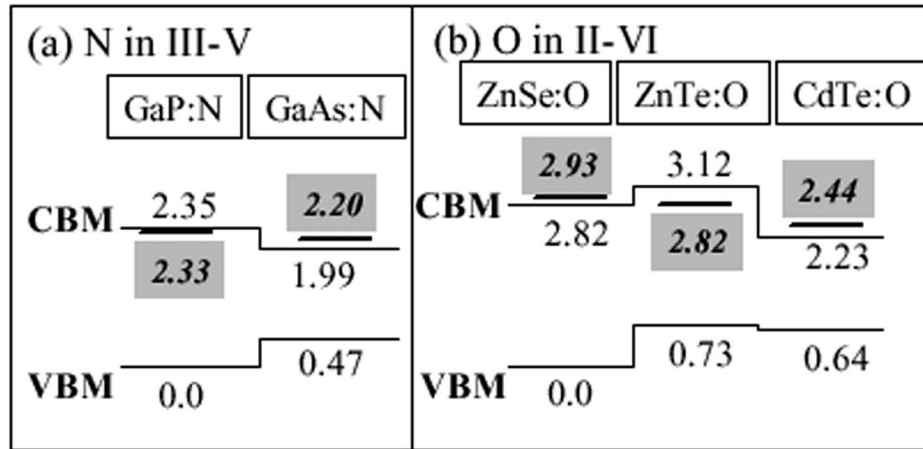


FIG. 1. Plot of the calculated band offsets and isovalent impurity levels (with gray background) in III-V and II-VI semiconductors. (a) N in GaAs and GaP; (b) O in ZnSe, ZnTe, and CdTe.

pecially for conduction band derived states such as in the case of CdTe:O. This is because for a partially localized state, it is not known how the defect level shifts with the band gap correction.

(2) The size of the system one can calculate self-consistently to date is limited to about a few hundred atoms, even when a large parallel computer is used. Previous tests have shown that the exact position of the isovalent impurity defect is very sensitive to the size of the system used in the calculation.<sup>17-19</sup> To overcome these difficulties associated with the conventional LDA calculation, large-cell and band gap corrected methods have to be used.

In this Rapid Communication, using a recently developed large scale plane-wave pseudopotential approach,<sup>17-20</sup> we perform systematic band structure and defect calculations to understand the chemical trends of the isovalent impurity level in semiconductors. We calculate oxygen induced isovalent levels in ZnSe:O, ZnTe:O, and CdTe:O, as well as the N level in the GaP:N and GaAs:N systems. We find that the position of the energy level is quite sensitive to the local environment around the oxygen atom in the II-VI system. The energy levels for the common-cation system tend to line up within 0.1 eV, because the local environment and the cation-O bond lengths are similar in common-cation systems. However, for common-anion systems the energy level position could be quite different. We find that the oxygen level in CdTe is about 0.4 eV lower than that in ZnTe, which is due to the large Cd-O bond length than the Zn-O bond length and the associated deformation potential.

In our calculation, the atomic structure of the defect, charge density  $\rho(\mathbf{r})$ , and the norm-conserving local pseudopotential  $V_{loc}(\mathbf{r})$  and nonlocal pseudopotential  $\hat{V}_{nonloc}(\mathbf{r})$  are obtained first by solving self-consistently the LDA Schrödinger's (Kohn-Sham) equation,<sup>21</sup>

$$\left[-\frac{1}{2}\nabla^2 + V_{loc}(\mathbf{r}) + \hat{V}_{nonloc}\right]\psi_i = \epsilon_i\psi_i. \quad (1)$$

The Zn 3d and Cd 4d electrons are included as valence electrons. A 65 Ry kinetic energy cutoff for the plane-wave basis set is used. The present plane-wave pseudopotential

LDA calculations give band gaps of 1.09, 0.77, 0.32, and 0.67 eV for bulk ZnSe, ZnTe, CdTe, and ZnO, respectively, smaller than the experimental value of 2.82, 2.38, 1.59, and 3.44 eV.<sup>22</sup> To correct this band gap error, we modified the potentials<sup>17-19</sup> of Zn, Cd, Se, Te, and O atoms by adding an external potential  $\beta \sin(r\pi/r_c)/r$  (zero outside  $r_c$ )<sup>23,24</sup> to the self-consistent nonlocal potential part in the final band structure calculations, where the parameters  $r_c$  and  $\beta$  are fitted to the band structure of bulk ZnX and CdX ( $X=O, Se, \text{ and } Te$ ). The fitted band gaps are 2.82, 2.38, 1.59, and 3.43 eV, respectively, for bulk ZnSe, ZnTe, CdTe, and ZnO, in good agreement with experimental data. The accuracy and transferability of this modified pseudopotential method have been tested extensively in the past for isovalent systems<sup>17,18</sup> and in present calculations. We find that for isovalent impurity and alloy systems, the calculated band structure obtained using this modified pseudopotential approach are in good agreement with available experimental data.

To calculate super-large systems, including supercells up to 4096 atoms, we use a recently developed “charge patching method” (CPM).<sup>20</sup> In the CPM, a 64 or 512 atom periodic cell is first calculated with the isovalent impurity at the center of this cell. The atoms within this medium size cell are fully relaxed using LDA quantum mechanical forces, except for the atoms at the cell surfaces, which are fixed at their ideal positions. For larger supercells with one impurity at the center, the charge density of the calculated medium size cell is patched to the outer region using the charge densities of pure bulk compounds. The generated charge density  $\rho(\mathbf{r})$  of the large supercell is then used to obtain the potential  $V(\mathbf{r})$  in Eq. (1). After that, Eq. (1) is solved using the folded spectrum method (FSM) (Ref. 25) for a few states near the band gap. In the FSM, the original Eq. (1)  $H\psi_i = \epsilon_i\psi_i$  is transferred to  $(H - E_{ref})^2\psi_i = (\epsilon_i - E_{ref})^2\psi_i$ , where  $E_{ref}$  is a pivot energy set to be inside the band gap. The details of the whole procedure can be found in Refs. 18 and 26.

Figure 2 shows the calculated energy levels of the  $a_1(O)$  and  $a_1(\Gamma_{1c})$  states as a function of the supercell size in the systems of (a) ZnSe:O, (b) ZnTe:O, and (c) CdTe:O. To analyze the wave-function character, we expand the wave func-

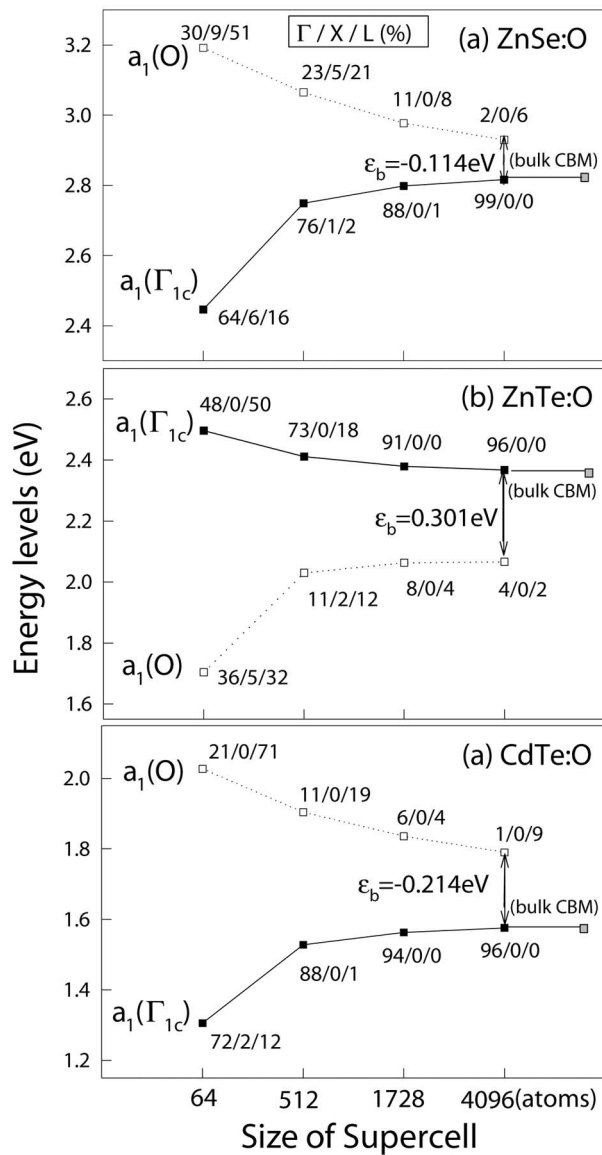


FIG. 2. Energy levels of the  $a_1(O)$  and  $a_1(\Gamma_{1c})$  states in (a) ZnSe:O, (b) ZnTe:O, and (c) CdTe:O as functions of the size of supercell. The percentages of  $\Gamma$ ,  $X$ , and  $L$  characters, respectively, for each state is also shown.

tion  $\psi_i$  in terms of Bloch states  $\{\phi_{n,k}\}$  of the bulk compounds. The spectral projection  $\sum_n |A_{n,k}|^2$  for  $\Gamma$ ,  $X$ , and  $L$  points are given in Fig. 2. We have the following findings.

(i) *Supercell size effect.* The calculated oxygen impurity level is very sensitive to the supercell size, reflecting the strong coupling between the impurities in different cells and coupling between different  $a_1$  states folded to the zone center through O-induced non-zinc-blende potential. We can define the single-particle impurity binding energy  $\epsilon_b$  as  $\epsilon_{CBM} - \epsilon_O$ , where  $\epsilon_{CBM}$  and  $\epsilon_O$  are the eigenenergies of the CBM and oxygen impurity state, respectively. If  $\epsilon_b$  is negative, the oxygen impurity level is above CBM, whereas if  $\epsilon_b$  is positive, the oxygen impurity level is below CBM. We find that  $|\epsilon_b|$  decreases as the cell size increases and becomes relatively converged for a 4096-atom supercell ( $8a \times 8a \times 8a$  cu-

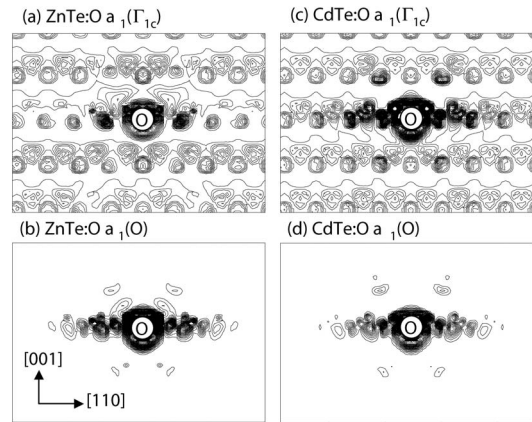


FIG. 3. The electron charge distribution of  $a_1(O)$  and  $a_1(\Gamma_{1c})$  states in ZnTe:O and CdTe:O systems.

bic box).  $|\epsilon_b|$  calculated using the 64-atom cell ( $2a \times 2a \times 2a$  cubic box) are poorly converged and can introduce an error in the order of about 0.5 eV. This is also reflected in the wave-function characters of the  $a_1(O)$  and  $a_1(\Gamma_{1c})$  states. For small 64-atom cell calculations, both levels are strongly hybridized with other folded  $a_1$  levels such as  $a_1(X)$  and  $a_1(L)$  states, and the percentages of  $\Gamma$  characters are in the same order for  $a_1(O)$  and  $a_1(\Gamma_{1c})$  states (Fig. 2). It is, therefore, difficult to identify the position of the  $a_1(O)$  bound state from the 64-atom calculations. For the large 4096-atom supercell calculation, the spectral projections show that the  $a_1(\Gamma_{1c})$  state becomes a nearly pure  $\Gamma$  state in the reciprocal space and the charge distribution in the real space is delocalized (Fig. 3); but the  $a_1(O)$  state becomes very delocalized in the reciprocal space with less than 5% contribution from the  $\Gamma$  point, and it is very localized in the real space around the oxygen atom (Fig. 3). It is interesting to note that the charge distribution of oxygen impurity states of ZnTe:O and CdTe:O (Fig. 3) are similar, with tails along the  $(110)$  direction, even though the  $a_1(O)$  state is a gap state in ZnTe:O and a resonant state inside the conduction band in CdTe:O (see below).

(ii) *Chemical trend of the isovalent impurity level.* From our large supercell calculation, we find that the calculated binding energy  $\epsilon_b$  of the isovalent oxygen impurity levels are  $-0.11$ ,  $0.30$ , and  $-0.21$  eV, respectively, in ZnSe:O, ZnTe:O, and CdTe:O systems, i.e., oxygen induces resonant impurity states inside the conduction band in ZnSe:O and CdTe:O, whereas it creates a localized impurity state below the conduction band in ZnTe:O. Using our calculated valence band offsets<sup>9</sup> and experimental band gaps<sup>22</sup> for these compounds, the absolute positions of these impurity levels are shown in Fig. 1(b). It shows that although the oxygen impurity level in ZnSe is only about 0.1 eV higher than that in ZnTe, the impurity level in CdTe is about 0.4 eV lower than that in ZnTe. This general trend is not sensitive to the fitting procedure used to correct the LDA band gap. We find that these results can be understood by noticing that although the  $a_1(O)$  state is quite localized on the oxygen site, its wave function actually has significant nearest neighbor cation characters [Figs. 3(b) and 3(d)]. Thus, the energy level of the defect level is strongly influenced by the nearest neighbor cation

atoms. As the impurity level has the antibonding conduction band character, its energy increases as the cation-O bond lengths decreases. Our calculated Zn-O bond lengths are  $d_0 = 2.08$  and  $2.10$  Å in ZnSe:O and ZnTe:O, respectively. This indicates that the Zn-O bond length is not sensitive to the anion atomic size, and thus explains why the O impurity level in ZnSe:O is only slightly higher than that in ZnTe:O. Similar results are obtained for GaAs:N and GaP:N systems [Fig. 1(a)]. However, the Cd-O bond length  $d_0 = 2.28$  Å in CdTe:O is much larger than the Zn-O bond in ZnTe:O due to the large Cd atomic size. Because  $a_1(O)$  is an antibonding state, its energy level decreases as the bond length increases.<sup>24</sup> This explains why the O impurity level in CdTe:O is lower in energy. This analysis also explains the results for GaP:N and GaAs:N systems [Fig. 1(a)]. Therefore, to a good approximation, the isovalent impurity levels line up in common-cation systems, but not in common-anion systems. The systems with large cation-O bond lengths also have lower O-impurity levels.

(iii) *Comparison with experimental measurements.* Our calculated binding energies  $\epsilon_b$  are  $-0.11$ ,  $0.30$ , and  $-0.21$  eV, respectively, for ZnSe:O, ZnTe:O, and CdTe:O at zero temperature. The RT experimental values are  $-0.22$ ,<sup>12</sup>  $0.24$ ,<sup>10</sup> and  $-0.4$  eV,<sup>11</sup> respectively, derived by fitting experimental optical data to the two-band anticrossing model. Because the energy of the localized impurity level is not sensitive to the temperature, whereas the CBM moves up in energy by about  $0.15$  eV from RT to zero temperature,<sup>27</sup> our calculated values, therefore, are in good agreement with ex-

perimental values. However, we must point out that the experimental values for ZnSe:O and CdTe:O were obtained by assuming that the O impurity levels align with those in ZnTe:O and used different band offsets than we calculated here.<sup>9</sup>

In summary, the isovalent oxygen impurity levels in II-VI semiconductors are studied using the state-of-the-art band structure method for supercells up to 4096 atoms per cell. The general chemical trends are revealed. The oxygen impurity level can exist either above CBM (ZnSe:O and CdTe:O) or below CBM (ZnTe:O). We explained that the generally accepted rule that isovalent localized O impurity levels in II-VI semiconductors are aligned in the absolute energy scale is true only if the impurity wave function was localized only at the O site. In reality, the impurity wave function extends to a longer range. If we include the contribution from the nearest neighbor atoms, then the impurity level would align only for common-cation systems such as the Zn compounds because it has the same O-Zn environment, but does not apply to the common-anion system such as ZnTe and CdTe because they have different O-Zn and O-Cd local environments. The systems with a large cation-O bond length also have lower O-impurity levels. Similar conclusion also applies to  $N$  isovalent impurity levels in III-V semiconductors.

The work is supported by the U.S. DOE under Contact No. DE-AC36-99GO10337. The use of computer resources of the NERSC is greatly appreciated.

<sup>1</sup>D. G. Thomas, J. J. Hopfield, and C. J. Frosch, Phys. Rev. Lett. **15**, 857 (1965).

<sup>2</sup>J. J. Hopfield, D. G. Thomas, and R. T. Lynch, Phys. Rev. Lett. **17**, 312 (1966).

<sup>3</sup>S.-H. Wei and A. Zunger, Phys. Rev. Lett. **76**, 664 (1996).

<sup>4</sup>J. D. Perkins *et al.*, Phys. Rev. Lett. **82**, 3312 (1999).

<sup>5</sup>H. P. Xin *et al.*, Appl. Phys. Lett. **76**, 1267 (2000).

<sup>6</sup>W. G. Allen, J. Phys. C **1**, 1136 (1968); **4**, 1936 (1971).

<sup>7</sup>J. C. Phillips, Phys. Rev. Lett. **22**, 285 (1969).

<sup>8</sup>D. J. Wolford *et al.*, in *Proceeding of the 17th International Conference on the Physics of Semiconductor*, edited by J. D. Chadi and W. A. Harrison (Springer, New York, 1984), p. 627.

<sup>9</sup>S.-H. Wei and A. Zunger, Appl. Phys. Lett. **72**, 2011 (1998).

<sup>10</sup>K. M. Yu *et al.*, Phys. Rev. Lett. **91**, 246403 (2003).

<sup>11</sup>K. M. Yu *et al.*, J. Appl. Phys. **95**, 6232 (2004).

<sup>12</sup>W. Shan *et al.*, Appl. Phys. Lett. **83**, 299 (2003).

<sup>13</sup>W. Shan *et al.*, Appl. Phys. Lett. **84**, 924 (2004).

<sup>14</sup>J. D. Cuthbert and D. G. Thomas, Phys. Rev. **154**, 763 (1967).

<sup>15</sup>M. J. Caldas, A. Fazzio, and A. Zunger, Appl. Phys. Lett. **45**, 671 (1984).

<sup>16</sup>C. G. Van de Walle and J. Neugebauer, Nature (London) **423**, 626 (2003).

<sup>17</sup>L.-W. Wang, Appl. Phys. Lett. **78**, 1565 (2001).

<sup>18</sup>J. Li and L.-W. Wang, Phys. Rev. B **67**, 033102 (2003).

<sup>19</sup>J. Li and L.-W. Wang, Phys. Rev. B **72**, 125325 (2005).

<sup>20</sup>L.-W. Wang, Phys. Rev. Lett. **88**, 256402 (2002).

<sup>21</sup>W. Kohn and L. J. Sham, Phys. Rev. **140**, A1133 (1965).

<sup>22</sup>*Semiconductors: Data Handbook*, 3rd ed., edited by O. Madelung (Springer, Berlin, 2004).

<sup>23</sup>N. E. Christensen, Phys. Rev. B **30**, 5753 (1984).

<sup>24</sup>S.-H. Wei *et al.*, Phys. Rev. B **67**, 165209 (2003).

<sup>25</sup>L.-W. Wang, A. Zunger, J. Chem. Phys. **100**, 2394 (1994).

<sup>26</sup>J. Li and L. W. Wang, Phys. Rev. B **67**, 205319 (2003).

<sup>27</sup>W. Walukiewicz *et al.*, Phys. Rev. Lett. **85**, 1552 (2000).